3D TUBULAR STRUCTURE EXTRACTION USING KERNEL-BASED SUPERELLIPSOID MODEL WITH GAUSSIAN PROCESS REGRESSION

Qingxiang Zhu, Dayu Zheng, Hongkai Xiong

Department of Electronic Engineering
Shanghai Jiao Tong University
Shanghai, 200240, China

ABSTRACT

To analyze the tubular structure correctly and obtain a record of the centerlines has become significantly more challenging and infers countless applications in a large amount of fields. Hence, a robust and automated technique for extracting the centerlines of the tubular structure is required. To address complicated 3D tubular objects, a novel kernel-based modeling approach with regard to minimizing tracking energy is presented in this paper. The 3D tubular structure can be demonstrated as a kernel-based superellipsoid model with non-uniform weights. To improve the performance, Gaussian process is also introduced to update the parameters of the kernel-based model, especially for the complicated structure with cross sections, varying radii, and complicated branches. At last, the extensive experimental results on 3D tubular data demonstrate that our proposed method deals effectively with complicated tubular structure.

***Index Terms*—** 3D tubular structure extraction, superellipsoid model, nonlinear prediction, Gaussian process

1. INTRODUCTION

This work is concerned with the problem of 3D tubular structure extraction. Of broad interest is the automated tracing and morphometry of tubular branched structures, e.g., neurons and blood vessels imaged by 3D microscopy. The difficulty of the tubular centerline extraction problem is due to its complicated structure, such as nearly circular cross sections, smoothly varying radii, and possibly complicated paths and branches. Therefore, there is a need of a robust and automated technique for extracting the tubular centerline and visualizing the underlying geometrical features and topological characteristics of the 3D tubular objects to ascertain the morphological properties and reconstruct the connectivity.

To describe the topological constraints in a geometric visualization way, a suitable model of the reconstructed tube is transformed by a linking line along center points. The relevant approaches proposed in the literature could be broadly classified into two categories, 2D-based and 3D-based.

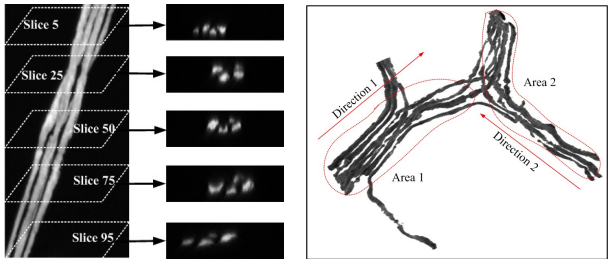

Fig. 1. A sample scenario of a 3D multi-temporal sequence of axons (a) A sketch map of 3D axon image stack. (b) MIP image of a 3D axon dataset.

In the early researches of 2D-based methods, the approaches are often involved with detecting targets in individual slices of 3D datasets and synthesizing correspondence between slices [1], which always make use of MIP (Maximum Intensity Projection). As shown in Fig. 1, the MIP image is generated from actual 3D axon dataset. Although far less computation is required than fully 3D-based approaches, those techniques suffer from incapability to detect and resolve truly 3D phenomena like cross sections, varying radii, and complicated branches. For the sake of avoiding the difficult dilemma, 3D based methods should be a better choice. Filter-based tracking method [2] aims to trace the tubular structure by successive filter responses of either the eigenvalue of the Hessian or the median core, however it is limited especially when contextual information is implicit, e.g. the discontinuous slices [3]. Several generalized cylinder kernels [4] [5] are introduced to preserve sufficient accuracy of tubular structure. A profound review can be found in [6]. However, the previous approaches have difficulties in handling the problems of cross sections, varying radii, and complicated branches which the proposed method focuses on.

In a first contribution of this paper, a kernel-based superellipsoid model is introduced to deal with the centerline extraction problem in 3D tubular structure. That is because the superellipsoid model has an explicit low-order parameterization with regard to the local pose of tubular segment, and

superellipsoid model is also insensitive to direction. Therefore, proposed superellipsoid model can cope with cross sections, varying radii, and complicated branches in 3D tubular structure. As a second contribution, the proposed approach takes into account the statistical correspondence of the kernel-based model using Gaussian process. Unlike the deterministic methods, the proposed approach can describe the nonlinear tracking model and handle the nonlinear problem. Therefore, Gaussian process (GP) [7] is utilized as a powerful tool for learning the regression function of the nonlinear tracking model, because of the advantages of Gaussian process, such as their modeling flexibility, ability to provide uncertain estimates, and ability to learn noise and smoothness parameters from training data.

The rest of the paper is organized as follows. Section 2 describes the Gaussian process for regression and our kernel-based Superellipsoid model. Section 3 details our 3D extraction problem formulation by using superellipsoid model with Gaussian process. Section 4 provides the experimental results on several axon sequences, and we conclude the whole work in Section 5.

2. SUPERELLIPSOID KERNEL WITH GAUSSIAN PROCESS

We first describe Gaussian process for regression in Sec. 2.1, and then introduce a superellipsoid kernel function utilizing Gaussian process in Sec. 2.2

2.1. Gaussian Process for Regression

Gaussian process is utilized for learning regression functions from sample data, which is a powerful and non-parametric tool. Modeling flexibility, the ability to provide uncertainty estimates and the capability to learn parameters from noisy training data are the three main advantages of Gaussian process. We assume that the set of training data is consisted of an M-dimensional input vector $x_i = [x_{i1}, x_{i2}, \cdots, x_{iM}]^T$ and a scalar output y_i derived from

$$y_i = \mathcal{G}(x_i) + \epsilon$$

where $\mathcal{G}(x_i)$ is a function with a Gaussian process prior, ϵ is white noise with variance σ_n^2. The vectorial inputs and scalar outputs are collected into $X = [x_1, x_2, \cdots, x_N]$ and $\mathcal{Y} = [y_1, y_2, \cdots, y_N]$, respectively. Therefore, the joint output follows a zero-mean multivariate Gaussian distribution.

$$\mathcal{Y} \sim N(0, K(X,X) + \sigma_n^2 I)$$

where $K(X,X)$ is the covariance matrix with elements $K_{ij} = k(x_i, x_j)$. The kernel function $k(x, x')$ is designed to measure similarity between the two inputs, which is commonly associated with a diagonal scale matrix W. The term $\sigma_n^2 I$ introduces the Gaussian noise derived from ϵ.

When the observation sample is noise-free, the prediction of Gaussian distribution can be simplified to gain the kernel function conditioned on the training data. Given training set $\mathcal{T} = \{X, \mathcal{Y}\}$, the Gaussian predictive distribution over test output y_* conditioned on test input x_* and $\mathcal{T}$ can estimate its mean and variance according to the kernels. In detail, the mean is estimated by

$$GP_\mu(x_*, X, \mathcal{Y}) = K(x_*, X)K(X,X)^{-1}\mathcal{Y}, \tag{1}$$

and the variance is

$$\begin{aligned} & GP_\Sigma(x_*, X, \mathcal{Y}) \\ = \; & K(x_*, x_*) - K(x_*, X)K(X,X)^{-1}K(X, x_*) \end{aligned} \tag{2}$$

where $K(x_*, X)$ measures the similarity between x_* and X. Therefore, the hyper-parameters of Gaussian process $\theta = [W, \mathcal{G}]$ describe the defined kernel functions. They can be given by pursuing the maximized conditional log-likelihood of the training outputs given the inputs,

$$\hat{\theta} = arg\max_\theta \{\log p(y|X, \theta)\} \tag{3}$$

which can be done using some numerical optimization techniques, e.g. conjugate-gradient descent.

2.2. Superellipsoid kernel function

Superellipsoids are the basis for a simple shape model that describes the localized tubular structure. Superellipsoids can be expressed as

$$(|x|^{\frac{2}{\epsilon_2}} + |y|^{\frac{2}{\epsilon_2}})^{\frac{\epsilon_2}{\epsilon_1}} + |z|^{\frac{2}{\epsilon_1}} = 1$$

where the parameters $\epsilon = (\epsilon_1, \epsilon_2)$ control the shape of the superellipsoid.

In order to establish an anisotropic tubular tracking model (3D tubular structure is anisotropic), the scale parameters $\delta = (\delta_1, \delta_2, \delta_3)$ are introduced into the superellipsoid model to describe the direction of tubular structure. Rather than considering a single isosurface as in [4], it will be convenient to work with the function

$$S(x) = \Big((\frac{x^{(1)}}{\delta_1})^{\frac{2}{\epsilon_2}} + (\frac{x^{(2)}}{\delta_2})^{\frac{2}{\epsilon_2}} \Big)^{\frac{\epsilon_2}{\epsilon_1}} + \Big(\frac{x^{(3)}}{\delta_3} \Big)^{\frac{2}{\epsilon_1}} \tag{4}$$

Note that Eq. (4) is a canonical superellipsoid form with parameters of scale, which is aligned with the coordinate axes and centered at the origin. The maximum likelihood center coordinate is in the major axis of superellipsoid. Therefore, the following kernel function is utilized in the proposed approach to track centerline points from the 3D tubular structure.

$$f(x,x') = \left(\left(\frac{x^{(1)}-x'^{(1)}}{\delta_1}\right)^{\frac{2}{\epsilon_2}} + \left(\frac{x^{(2)}-x'^{(2)}}{\delta_2}\right)^{\frac{2}{\epsilon_2}} \right)^{\frac{\epsilon_2}{\epsilon_1}} + \left(\frac{x^{(3)}-x'^{(3)}}{\delta_3}\right)^{\frac{2}{\epsilon_1}} \quad (5)$$

In order to deal with discontinuous structure and varying radii, the Gaussian process is utilized to update the parameters of the proposed superellipsoid model.

$$f(x,GP) = \left(\left(\frac{x^{(1)}-GP_{\mu}^{(1)}}{GP_{\Sigma}^{(1)}}\right)^{\frac{2}{\epsilon_2}} + \left(\frac{x^{(2)}-GP_{\mu}^{(2)}}{GP_{\Sigma}^{(2)}}\right)^{\frac{2}{\epsilon_2}} \right)^{\frac{\epsilon_2}{\epsilon_1}} + \left(\frac{x^{(3)}-GP_{\mu}^{(3)}}{GP_{\Sigma}^{(3)}}\right)^{\frac{2}{\epsilon_1}} \quad (6)$$

where the parameters ϵ_1, ϵ_2 are allowed to control the shape curvature, GP_{μ} is calculated by Eq. (1), which is the predicted center of the superellipsoid kernel, and GP_{Σ} is calculated by Eq. (2), which is the scale factor vector in the 3D kernel. This compact model permits to handle a large variety of shapes, including: ellipsoid for $\epsilon_1 = \epsilon_2 = 1$, parallelepiped for $\epsilon_1 \to 0$ and $\epsilon_2 \to 0$, cylinder for $\epsilon_1 \leq 1$ and $\epsilon_2 = 1$, and so on. Hence, the superellipsoid is in a form of a spheroid (either oblate or prolate spheroid), and the solid body is an ellipsoid.

In the proposed problem of tubular structure extraction, the superellipsoid model is simplified for a strict shape constraint. In order to adapt the model to the tubular structure extraction and reduce the computational complexity, the shape parameter ϵ_2 is set to unity. Hence, a new canonical form of the superellipsoid isosurface with a fixed shape is described

$$f(x,GP) = \left(\left(\frac{x^{(1)}-GP_{\mu}^{(1)}}{GP_{\Sigma}^{(1)}}\right)^{2} + \left(\frac{x^{(2)}-GP_{\mu}^{(2)}}{GP_{\Sigma}^{(2)}}\right)^{2} \right)^{\frac{1}{\epsilon}} + \left(\frac{x^{(3)}-GP_{\mu}^{(3)}}{GP_{\Sigma}^{(3)}}\right)^{\frac{2}{\epsilon}} \quad (7)$$

where GP_{μ} is the center of the superellipsoid kernel, and GP_{Σ} is the scale factor vector on x, y, and z axis in the 3D kernel, respectively.

3. 3D TUBULAR STRUCTURE EXTRACTION PROBLEM FORMULATION

Firstly, we have to clarify some basic factors in tubular structure extraction problem. The ridge (highest grey level) of a tube usually occurs at the center, and the radius of the tube is based on variance, even if a single tube might have different radii along its axis.

Aylward and Bullitt [2] use a "shifted normal plane to follow the ridge. The "shifted normal plane can provide a quick response to shape change of tubular structure but requires additional algorithm to determine plane's normal direction. The calculation of normal direction is relatively complicated and precise accuracy is demanded to ensure the validity of tracking. To avoid calculating normal direction and thus ensure the validity of tracking, we choose superellipsoid model to cope with 3D tubular structure extraction problem. As shown in Fig. 2, superellipsoid is insensitive to direction, so that the calculation of normal direction is not required any more.

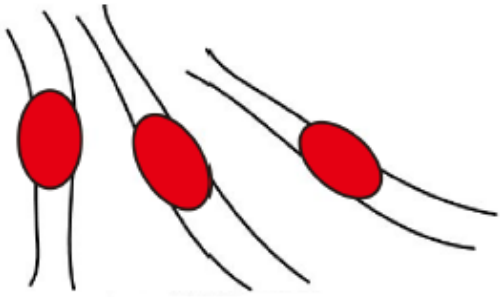

Fig. 2. Example of using superellipsoid model to extract tubular structure. Normal direction is not calculated any more.

Therefore, we introduced an superellipsoid traversing algorithm to deal with the tubular extraction problem. We initialized the algorithm by placing a superellipsoid model into the tubular structure, smaller enough not to touch the tube surface. Besides that, if the tubular structure's orientation is unknown, we should assume that touching may occur at any directions when designing the centerline extraction algorithm. In order to get the same response to touching on various orientations, superellipsoid is the most reasonable choice.

According to our common sense, the extracted centerline point should be located at where the pixel intensity is relatively high, and also close to the predicted position based on the previous centerline points and the direction of the tube.

The original image stack contains a voxel set V and we define an intensity query function $I(v)$ ($v \in V$), which represents the intensity of the pixel at v. Assuming the image stack contains N different tubes, the trajectory of the centerline of the nth tubular structure is denoted as c_n ($n \in [1, 2, \cdots, N]$), and the point of the centerline in the ith step (in the image stack) is denoted as $c_n^{(i)}$, the tracking vector between $c_n^{(i)}$ and $c_n^{(i-1)}$ in the ith step is denoted as $d_n^{(i)} = c_n^{(i)} - c_n^{(i-1)}$.

To achieve a better extraction result of the centerline points, we establish an energy function shown in Eq. 8, which consists of two terms: the data term and the smoothness term. The data term measures the consistency between the extracted centerline point and the previous centerline points, while the smoothness term enforces spatial coherence.

$$E_n^{(i)} = \Phi(c_n^{(i)}) + \eta\Psi(d_n^{(i)}) \quad (8)$$

where $\Phi(c_n^{(i)})$ is the data term measures the disagreement between the current centerline point and the previous ones, and

$\Psi(d_n^{(i)})$ is the smoothness term which penalizes the sudden change in the consecutive search directions and preserves the spatial coherence of the centerline of tubular structure, and η is a factor to balance the weight between the two terms.

We will elaborate the two terms in the following.

$$\Phi(c_n^{(i)}) = (1 - I(c_n^{(i)}))f\big(c_n^{(i)}, GP(c_n^{(i)})\big) \tag{9}$$

where $I(c_n^{(i)})$ is the pixel intensity at $c_n^{(i)}$, $f\big(c_n^{(i)}, GP(c_n^{(i)})\big)$ is the kernel function described in Eq. (7), and $GP(c_n^{(i)})$ is a Gaussian process prediction based on $\{c_n^{(1)}, ..., c_n^{(i-1)}\}$.

$$\Psi(d_n^{(i)}) = f\big(d_n^{(i)}, GP(d_n^{(i)})\big)e^{arccos\frac{d_n^{(i)} \cdot GP_\mu(d_n^{(i)})}{||d_n^{(i)}|| \cdot ||GP_\mu(d_n^{(i)})||}} \tag{10}$$

where $d_n^{(i)} = c_n^{(i)} - c_n^{(i-1)}$, $f\big(d_n^{(i)}, GP(d_n^{(i)})\big)$ is also the kernel function described in Eq. (7), and $GP(d_n^{(i)})$ is a Gaussian process prediction based on $\{d_n^{(1)}, ..., d_n^{(i-1)}\}$.

In Eq. (9), we can see that when extracted centerline point $c_n^{(i)}$ has higher pixel intensity, $(1 - I(c_n^{(i)}))$ gets a smaller value. And the kernel function $f\big(c_n^{(i)}, GP(c_n^{(i)})\big)$ achieves small value when $c_n^{(i)}$ is consistent with the Gaussian process prediction $GP(c_n^{(i)})$. In Eq. (10), $arccos\frac{d_n^{(i)} \cdot GP_\mu(d_n^{(i)})}{||d_n^{(i)}|| \cdot ||GP_\mu(d_n^{(i)})||}$ is actually the angle between vector $d_n^{(i)}$ and $GP_\mu(d_n^{(i)})$. Larger difference in angle will increase the value of $\Psi(d_n^{(i)})$. In order to obtain accurate centerline points from the whole image stack, we can solve the following optimization problem.

$$\begin{aligned} & \min_{c_n^{(i)}} \textstyle\sum_n \sum_i \big(\Phi(c_n^{(i)}) + \eta\Psi(d_n^{(i)})\big) \\ s.t. \quad & c_n^{(i)} \in S(c_n^{(i-1)}) \\ & c_n^{(i)} \notin \{c_n^{(1)}, c_n^{(2)}, \cdots, c_n^{(i-1)}\} \end{aligned} \tag{11}$$

where $S(c_n^{(i-1)})$ is the superellipsoid kernel space in 3D volume which is defined in Eq. (4).

Therefore, we can easily obtain the tubular centerline by solving the optimization problem to search the candidate directions around the maximum likelihood direction $GP_\mu(d_n^{(i)})$ and maximize the tracking energy as defined in Eq. (11).

Noise and interference is inevitable in original dataset. To reduce or eliminate such affection, the radius of the superellipsoid should be carefully designed. As shown in Fig. 3(a) where a noise point with high gray level intensity occurs in the image data, the superellipsoid will be trapped by the noise dot if the radius is too low. A lower bound of superellipsoid's radius can be derived by statistical properties of noise and interference. Also, if the radius is too large, the tracking ability will fade quickly at the twisted parts of target axons and lose details as shown in Fig. 3(b).

There are two major factors we need to take into consideration when seeking an optimal radius for the superellipsoid:

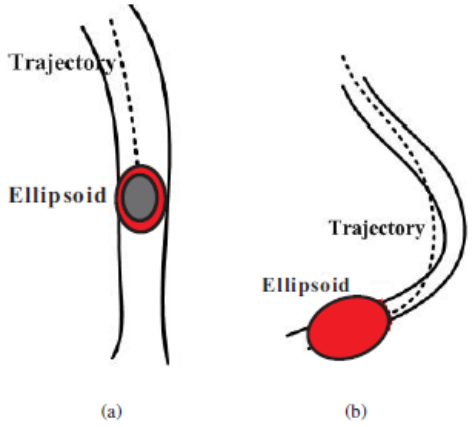

Fig. 3. Lower bound and upper bound of superellipsoid's radius, (a) Superellipsoid will be trapped in noise with high gray level intensity if radius is too small; (b) Details will lost if the radius is too large.

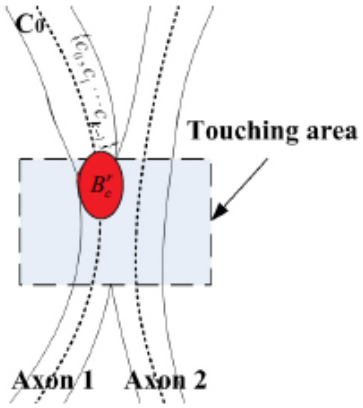

Fig. 4. Sketch map of touching problem

(a) noise and interference in the target dataset, and (b) radius interval of target tubular structure. Factor (a) gives a lower bound constraint for the superellipsoid parameters while factor (b) gives an upper one. Since the radius of the superellipsoid model is hard to choose, Gaussian process is utilized for estimation. The mean and variance are the center and radius of superellipsoid model respectively.

Our proposed can also deal with touching problems, which can be viewed as two close-lying tubes with similar gray level intensities as shown in Fig. 4. Touching is hard to solve since traditional methods require a clear boundary to perform tracking which is not available in touching area. Although there is no clear boundary, the centerline of the tubular structure where gray level intensity reaches local maximum remains clear and independent even in touching area. This

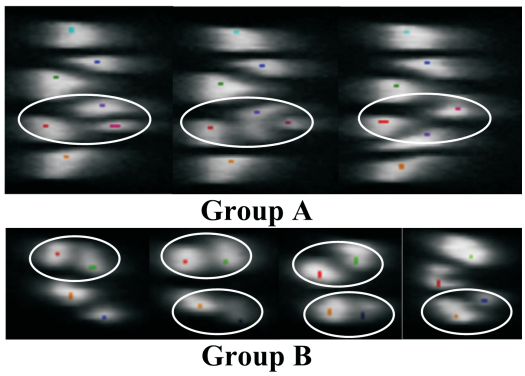

Fig. 5. The touching cases in image data

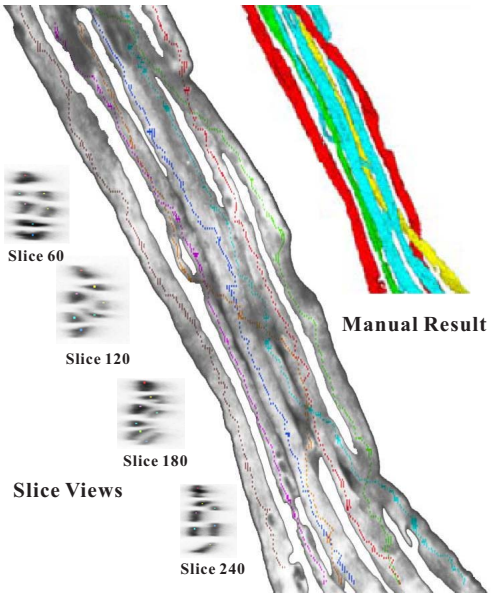

Fig. 6. Centerline extraction results of tubular structure with varying radii.

property indicates that touching problem can be solved if the tracking result is accurate enough to ensure the trajectory of centerline is very close to the real centerline.

Two groups of slices of touching axons are shown in Fig. 5. It can be noted that our scheme is able to choose the correct part of the touched axons although axons are twisted and there is no palpable boundary in some slices.

4. EXPERIMENTAL RESULTS

To validate the efficiency of the approach, we applied the proposed approach on a large number of real axon image stacks with complicated structure. Fig. 6 shows an image volume with varying radii, and Fig. 8 with cross sections and discontinuous structure. Both of the image volumes contain several tubes through 256 image slices. We initialized GP_μ manually

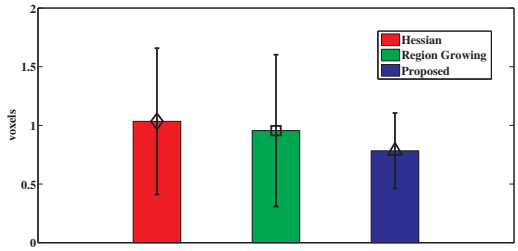

Fig. 7. Statistical mean errors and standard deviations in three methods (Hessian kernel [2], region growing [8] and the proposed).

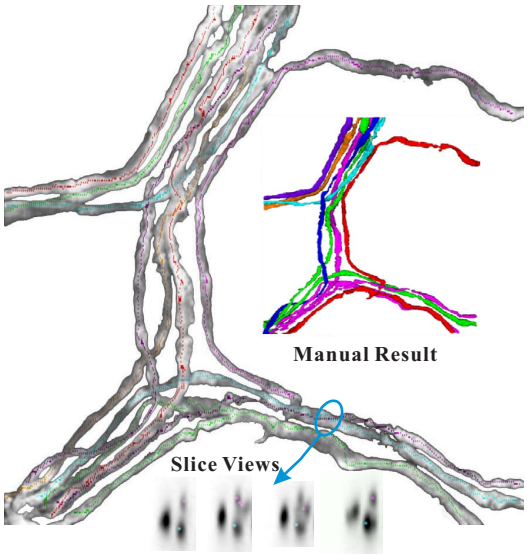

Fig. 8. Centerline extraction results of tubular structure with cross sections and discontinuous structure.

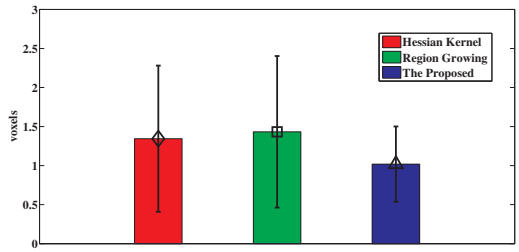

Fig. 9. Statistical mean errors and standard deviations in three methods (Hessian kernel [2], region growing [8] and the proposed).

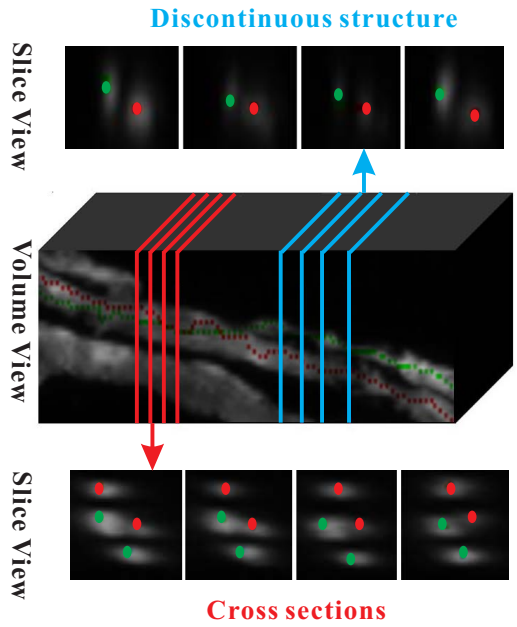

Fig. 10. Results of discontinuous structure and cross sections.

and set GP_Σ in three axes as $[1, 1, 1]$. The energy balance weight η is 10 in all our experiments. It is shown that the proposed approach can deal with complicated tubular structure very well, even though the image data is full of the curvilinear and branch structure, e.g. some sampled slices. It is clear that the proposed approach is capable of tracking the centerlines of the tubular structure, and dealing with cross sections, varying radii, and complicated branches. Manual results are also provided for verification.

The statistical results of the three different tubular structure extraction methods are demonstrated in Fig. 7 and Fig. 9, i.e., Hessian kernel [2], region growing [8], and the proposed one. The error is defined as the minimum distance between the predicted centerline voxels and the ground truth centerline voxels. It is obvious that both the mean and the standard deviation of errors between the results using the proposed method and ground truth is the smallest one of the three methods.

In detail, the cross sections and discontinuous structure of the image data are discussed in Fig. 10, which demonstrates the common complicated cases as part of the axon image stack in Fig. 8. Due to the proposed approach with adaptive parameters updated by Gaussian process, the proposed approach can easily handle a large amount of the complicated cases. Finally, we evaluated the proposed method on another two 3D tubular image stacks, shown in Fig. 11.

5. CONCLUSIONS

This paper introduced a novel tubular structure central axis extraction approach, which is composed of the following aspects: a superellipsoid model for tubular structure tracking and Gaussian process for predicting evolution of the centerline. We have shown the validity of our scheme against a variety of interferences and the ability of dealing with touching and twisting problems which are the major issues within tubular structure extraction. The extraction is highly automated, rapid, and accurate, making it suitable for replacing the fully manual methods of extracting complicated structures when studying the 3D tubular image sequences.

Fig. 11. More 3D tubular experimental results.

6. REFERENCES

[1] H. Cai, X. Xu, and J. Lu, et. al., "Repulsive force based snake model to segment and track neuronal axons in 3D microscopy image stacks," *NeuroImage*, vol. 32, no. 4, pp. 1608-1620, 2006.

[2] S. Aylward, and E. Bullitt, "Initialization, noise, singularities, and scale in height ridge traversal for tubular object centerline extraction," *IEEE Trans. Med. Imaging*, vol. 21, no. 2, pp. 61-75, 2002.

[3] Y. Kang, K. Engelke, W. Kalender, "A new accurate and precise 3-D segmentation method for skeletal structures in volumetric CT data," *IEEE Trans. Med. Imaging*, vol. 22, no. 5, pp. 586-598, 2003.

[4] J. Tyrrell, E. Tomaso, and D. Fuja, et. al., "Robust 3-D Modeling of Vasculature Imagery Using Superellipsoids," *IEEE Trans. Med. Imaging*, vol. 26, no. 2, pp. 223-237, 2007.

[5] V. Mohan, G. Sundaramoorthi, and A. Tannenbaum, "Tubular Surface Segmentation for Extracting Anatomical Structures From Medical Imagery", *IEEE Trans. Med. Imaging*, vol. 29, no. 12, pp. 1945-1958, 2010.

[6] A. Huang, H. Liu, and C. Lee, et. al., "On Concise 3-D Simple Point Characterizations: A Marching Cubes Paradigm", *IEEE Trans. Med. Imaging*, vol. 28, no. 1, pp. 43-51, 2009.

[7] C. E. Rasmussen, and C. K. I. Williams, "Gaussian processes for machine learning", *The MIT Press*, 2006.

[8] K. Zhang, H. Xiong, X. Zhou, and S. Wong, "A 3D self-adjust region growing method for axon extraction", in *Proc. IEEE Int. Conf. Image Proc.*, vol. 2, pp. 433-436, 2007.